References

AURIVILLIUS, B. (1964). *Acta Chem. Scand.* **18**, 1823.
AURIVILLIUS, B. & MALMROS, G. (1972). *Trans. R. Inst. Technol. Stockholm*, **291**, 545–562.
BALLESTRACCI, M. R. (1967). *C.R. Acad. Sci.* **264**, 1736–1738.
BOLLER, H. (1973). *Monatsh. Chem.* **104**, 916–919.
CROMER, D. T. & MANN, J. B. (1968). *Acta Cryst.* **25**, 321–323.
FINGER, L. W. (1969). *RFINE2*. Geophysical Laboratory, Carnegie Institution, Washington, DC.
IITAKA, Y. & NOWACKI, W. (1962). *Acta Cryst.* **15**, 691–698.
International Tables for X-ray Crystallography (1974). Vol. IV. Birmingham: Kynoch Press.
KUPČÍK, V. (1967). *Naturwissenschaften*, **54**, 114.

KUPČÍK, V. & NOVÁKOVÁ, L. V. (1970). *Tschermaks Mineral. Petrogr. Mitt.* **14**, 55–59.
MALMROS, G. (1970). *Acta Chem. Scand.* **24**, 384–396.
OHMASA, M. & NOWACKI, W. (1970). *Z. Kristallogr.* **132**, 71–86.
PORTHEINE, J. C. & NOWACKI, W. (1975). *Z. Kristallogr.* **141**, 387–402.
SILLÉN, L. G. (1939). *Z. Anorg. Allg. Chem.* **242**, 41.
SILLÉN, L. G. (1941). *Z. Anorg. Allg. Chem.* **246**, 115.
SILLÉN, L. G. & HUSBERG, G. (1941). *Z. Anorg. Allg. Chem.* **248**, 121.
WUENSCH, B. J. & PREWITT, C. T. (1965). *ACACA*. Absorption correction program.
ZACHARIASEN, W. H. (1949). *Acta Cryst.* **2**, 291–296.

Electron-Microscopic Study of the Structure of a Metastable Oxide Formed in the Initial Stage of Copper Oxidation. I. Cu4O

BY R. GUAN,* H. HASHIMOTO AND T. YOSHIDA

Department of Applied Physics, Osaka University, 2-1 Yamadaoka, Suita, Osaka 565, Japan

Abstract

In an early stage of oxidation of copper, a metastable copper oxide with the chemical composition Cu_4O has been observed by an atomic-resolution electron microscope. The atomic positions of Cu and O have been studied using electron-microscope images and diffraction patterns interpreted by calculations based on the dynamical theory of electron diffraction. The unit cell of the new oxide Cu_4O belongs to the orthorhombic system with space group $Pmm2$. The lattice parameters are $a = 4\cdot02$, $b = 5\cdot66$ and $c = 5\cdot94$ Å. The volume is approximately two times larger than that of Cu_2O. It is pointed out that at a certain thickness the images of O atoms appear bright and those of Cu atoms do not.

1. Introduction

In the early stages of oxidation of nickel single crystals, Garmon & Lawless (1966) found the existence of an induction period prior to the formation of nickel oxide, which was confirmed by structural changes in the nickel films. They observed a superlattice diffraction pattern similar to that found by Alessandrini & Freedman (1963) for the ordered structures of oxygen in nickel. In the case of copper, Ishii & Hashimoto (1967) observed a superlattice diffraction pattern which seems to be due to a structure intermediate

between cuprous oxide and cupric oxide. More recent studies of the oxidation of copper [for a summary see Howie (1981, 1983)] have shown a number of adsorbed-oxygen ordered structures leading after an induction period to the formation of Cu_2O nuclei sometimes with a covering of CuO. Shibahara & Hashimoto (1980) observed a tungsten oxide crystal with a smaller content of oxygen than in WO_2, formed when WO_3 crystals were evaporated in a vacuum of 10^{-4} Pa.

In order to study the non-stoichiometric copper oxide structure observed by Ishii & Hashimoto (1967), the present authors have carried out further observations of the initial stages of copper oxidation and found a new type of copper oxide containing less oxygen than Cu_2O. In this observation, the copper oxide is sometimes found together with its superstructure. The atomic structure has been analysed using a high-resolution transmission electron microscope with interpretation based on the many-beam dynamical theory of electron diffraction. The present paper is concerned with the atomic structure of an oxide having the chemical composition Cu_4O.

2. Specimen preparation and observation

Specimens were prepared in a way similar to that described by Ishii & Hashimoto (1967). A block of pure copper (purity about 99·99%) was rolled into a sheet 70 μm thick. The sheet was annealed at about 923 K in a vacuum of 2·66 Pa for 30 min, and was then electrolytically thinned by a window method in

---

* Visiting Researcher (1981–1982), on leave of absence from the Institute of Metal Research, Academia Sinica, Shenyang, China.

nitric acid and methyl alcohol. The thin films were then oxidized at $770 \sim 820$ K in a vacuum of $2 \sim 2 \cdot 4$ Pa for about 2 min. The observations of the atomic structure of the oxidized films were also carried out in a vacuum of $10^{-1} \sim 10^{-3}$ Pa in the electron microscope at 770–820 K under electron-beam irradiation. During the *in situ* observation of oxidation, when the oxide film was formed on the surface of the copper specimen, some parts of the copper were evaporated together with the oxide layer but other parts of the oxide layer remained. This phenomenon is similar to that observed by Ishii & Hashimoto (1967). The evaporation of copper may be due to the elevation of the specimen temperature during oxidation. A low-magnification electron-microscope image from such a film is shown in Fig. 1. The dark part in this figure is the copper matrix probably covered with copper oxide with a thickness of several hundred Å. The copper oxide crystal which is indicated by a circular mark at the center of Fig. 1 has a ribbon shape of thickness 100–200 Å and with other dimensions about 2000×7000 Å. The crystals are connected by a thin amorphous layer less than 50 Å thick. Fig. 2 shows high-magnification images of a ribbon-shaped oxide film. As can be seen in Fig. 2(*a*) and the interpretation given in Fig. 2(*b*), the oxide film consists of regions *A* and *B* which are separated by a grain boundary (*G.B*) and superstructure (*S.S*) is seen in region *B*. Figs. 2(*c*), 2(*d*) and 2(*e*) are magnifications of the regions indicated by (*C*), (*D*) and (*E*) in Fig. 2(*b*), respectively; here the grain boundary and superstructure are shown in (*c*), region *B* in (*d*) and region *A* in (*e*).

The electron diffraction pattern corresponding to the area shown in Fig. 2(*a*) is shown in Fig. 3(*a*) together with an explanation in Fig. 3(*b*). The diffraction pattern suggests that a crystal with a unit cell similar to that of Cu_2O is arranged in two orientations, *i.e.* (011) and (001) are parallel to the crystal surface as shown in Fig. 3(*c*). It seems reasonable that the oxide formed is parallel to planes (011) and (001), because the substrate copper was rolled into a sheet and hence planes (011) and (001) of copper are parallel to the specimen surface and the Cu_2O crystal will grow epitaxially on the surface of the copper crystal, *i.e.* (011) and (001) of the Cu_2O crystal are parallel to the specimen surface. Since the intensity of the electron diffraction spots cannot be completely explained by a Cu_2O crystal, there may be some anomalies in the composition of the atoms, and hence we tentatively name this crystal Cu_2O'. Determination of the position of the Cu and O atoms in the Cu_2O' crystal was carried out by comparing the observed intensity distribution of the electron-microscope images and the electron diffraction pattern with the theoretical calculation by the many-beam dynamical theory of electron diffraction. The procedure for atomic structure determination is described in § 3. The details of the superstructure are not discussed in this paper.

3. Crystal structure

The perspective view of a unit cell of Cu_2O is given in Fig. 4(*a*) and the (110) projection is shown in Fig. 4(*b*). Figs. 4(*c*) and 4(*d*) are the calculated intensity


Fig. 1. Copper oxide film, formed on the surface of a thin copper crystal by heating at 770–820 K in a vacuum of $2 \sim 2 \cdot 4$ Pa for 2 min. Some parts of the oxide region have evaporated. The thickness of the film indicated by a circle is $100 \sim 200$ Å.

distributions of electron waves at the bottom face of Cu_2O in the orientation shown in (b) with film thicknesses of 120 and 150 Å, respectively. The calculated contrast does not change with a change of thickness of ±10 Å. In Fig. 4(c), the large white discs represent the images of O atoms, while the images of Cu atoms are represented by small white discs. In Fig. 4(d), however, only the images of the O atoms can be observed and the images of the Cu atoms disappear. Carrying out the calculation of the theoretical intensity distribution at the bottom face of the Cu_2O crystal with various thicknesses up to 500 Å, we noted that though the images of O atoms are always observed clearly, the images of Cu atoms are very sensitive to the film thickness and often disappear. By comparing the electron micrograph shown in Fig. 2(e)
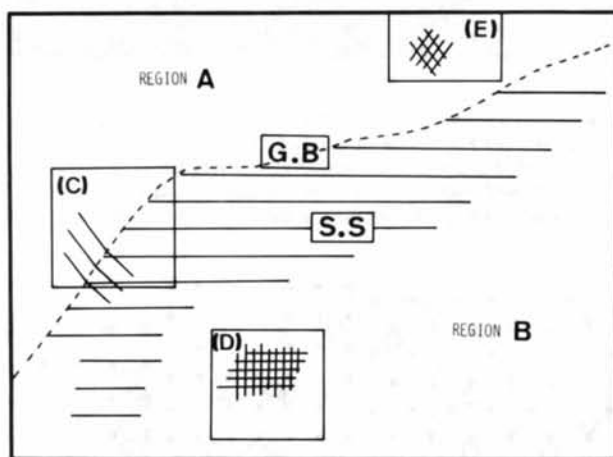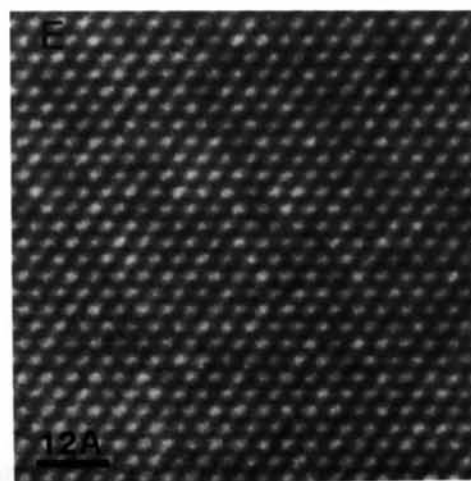

(c)

(a)

(d)

(b)
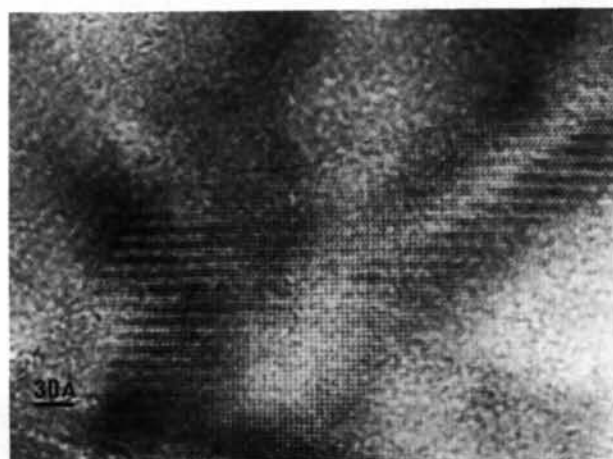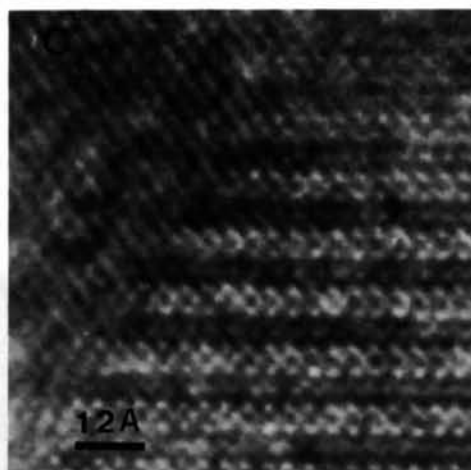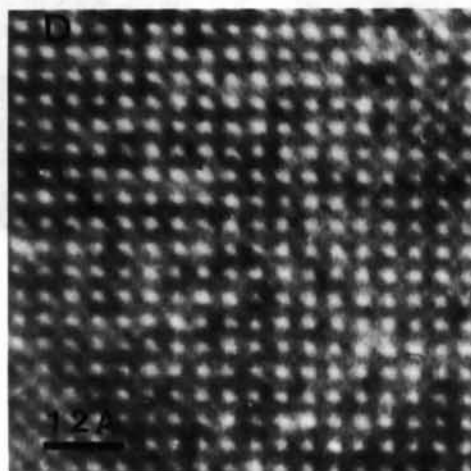
Fig. 2. (a) Larger magnification of part of Fig. 1. (b) Explanation of (a). Regions A and B on either side of the grain boundary (G.B) show atomic structure. A superstructure (S.S) is seen in region B.

(e)

Fig. 2 (cont.). (c), (d), (e) Magnifications of the regions indicated by (C), (D), (E) in (b).

and the calculated image shown in Fig. 4(d), it is seen that the bright spots in Fig. 2(e) correspond to every other bright spot in Fig. 4(d). Therefore, it is assumed that the projection of the atomic structure shown in Fig. 5(a) and (b) is that for the Cu_2O' crystal in [110] and [100] orientations of the Cu_2O lattice. One of the O atoms in the unit cell of Cu_2O is eliminated and the position of the other O atom is changed, which
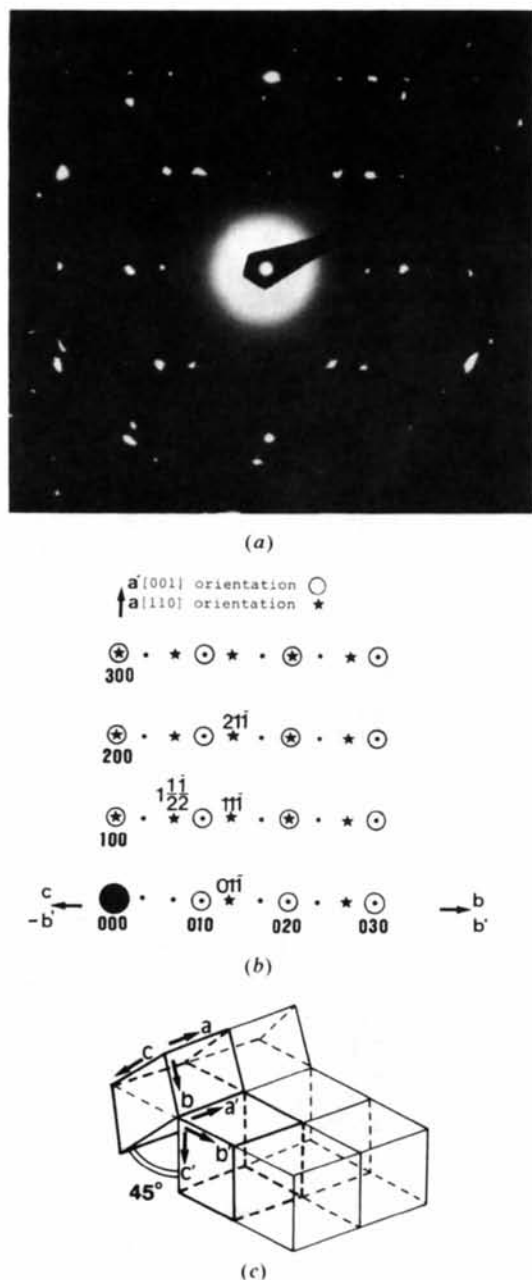
can be seen by referring to the positions of atoms in Cu_2O shown in Fig. 5(c). In this model, the oxide has the chemical composition Cu_4O and can no longer be described by the unit cell of Cu_2O, and thus a new unit cell is constructed as shown by the full lines in Fig. 5(a) and (b). The relation between the unit cell of Cu_2O and that of the new model of Cu_4O is shown in Fig. 6(a) which corresponds to Fig. 3(c). The axes of the unit cell of Cu_4O which are projected in the planes shown in Fig. 3(b) are shown in Fig. 6(b) together with the reciprocal nets projected on to (001) and (100).

In the unit cell of Cu_4O, there are eight Cu atoms with the coordinates $(0, 0, 0)$, $(0, \frac{1}{2}, 0)$, $(0, 0, \frac{1}{2})$, $(0, \frac{1}{2}, \frac{1}{2})$, $(\frac{1}{2}, \frac{1}{4}, \frac{1}{4})$, $(\frac{1}{2}, \frac{3}{4}, \frac{1}{4})$, $(\frac{1}{2}, \frac{1}{4}, \frac{3}{4})$, $(\frac{1}{2}, \frac{3}{4}, \frac{3}{4})$ and two O atoms with the coordinates $(\frac{1}{4}, \frac{1}{4}, 0)$, $(\frac{1}{4}, \frac{1}{4}, \frac{1}{2})$. This crystal of Cu_4O belongs to the orthorhombic system with lattice constants $a = 4\cdot02$, $b = 5\cdot66$ and $c = 5\cdot94$ Å. The space group is assigned as $Pmm2$ from crystallographic consideration of the proposed structure model.

(a)

a′[001] orientation ○
a[110] orientation ★

(b)

(c)

Fig. 3. (a) Electron diffraction pattern corresponding to Fig. 2(a). (b) Explanation of (a). ○ and * represent the spots from the Cu_2O crystal in [001] and [011] orientations ([001] and [011] are parallel to the incident beam). • represents a superstructure spot. (c) Perspective view of Cu_2O crystals in [001] and [011] orientations which give the diffraction pattern shown in (a).
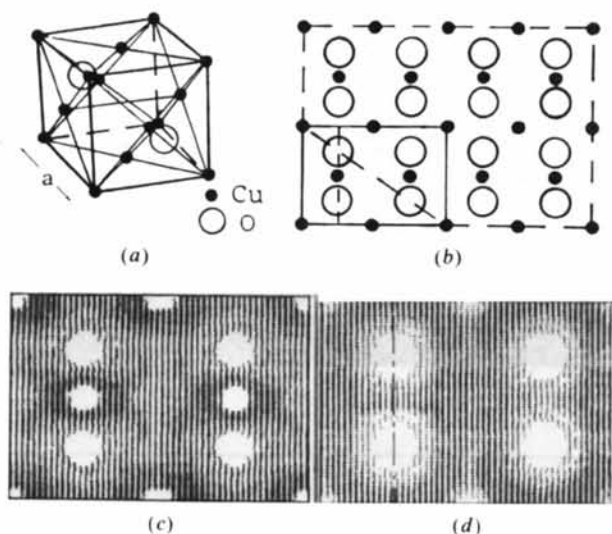

Fig. 4. (a) Perspective view of a unit cell of Cu_2O ($a = b = c = 4\cdot27$ Å). (b) Projection of Cu and O atoms onto (110). (c), (d) Calculated intensity distribution of electron waves at the bottom face of the Cu_2O crystal in [110] orientation, with thicknesses of 120 and 150 Å, corresponding to the area shown in (b) with a full line.
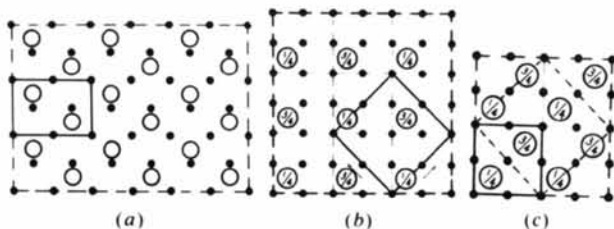

Fig. 5. (a) and (b) show the projection of Cu and O atoms of the proposed model of Cu_2O' (Cu_4O) onto (110) and (100). (c) Projection of atoms of the Cu_2O crystal onto (100). Numbers at O-atom positions represent the heights.

4. Comparison of the calculations with the observations

The model of Cu_4O has been confirmed by a comparison of the image observations with the intensity distribution of electron waves at the bottom face of the crystal or with the electron diffraction pattern calculated using the multislice method of the dynamical theory of electron diffraction.

First, amplitudes and intensities of diffracted waves from the various lattice planes of the Cu_4O crystal in [001] and [100] orientations with various thicknesses were calculated and the thickness dependence of the amplitudes of several main diffracted waves from the crystal in the [001] orientation is shown in Fig. 7(a). As can be seen in Fig. 7(a), though the amplitudes from (100), (110), (101), (020) and (002) increase gradually with increasing thickness, the amplitudes from (000), (120), (102) and (200) oscillate with a period of about 100 Å.

The calculated intensity of the electron diffraction patterns from the Cu_4O crystal in [001] orientation is shown in Fig. 7(b) for thicknesses of 216, 274 and 386 Å. The pattern from the crystal 216 Å thick agrees well with the observed diffraction pattern shown in Fig. 3(a), whose indices are shown in Fig. 6(b).

The calculated images at the bottom face of the crystals are shown in Fig. 7(c) for the thicknesses 110, 216, 274 and 386 Å. It should be noted that the calculated image for a thickness of 110 Å is the same as that for a thickness of 216 Å, and the image for a thickness of

274 Å is the same as that for 386 Å. For the thicknesses 274 and 386 Å, the image of O (large white disc) and the image of Cu (small white disc) can be observed simultaneously, but for the thicknesses 110 or 216 Å only the image of O can be observed.

Since the amplitudes of the diffracted waves from (200), (102) and (120), which reflect the periodicity of the arrangement of copper, become minima at the thicknesses 110 and 216 Å, as can be seen in Fig. 7(a), the images of Cu atoms disappear at these thicknesses. On the other hand, the diffracted waves from (110) and (101) which contain O, always have some magnitude and above 150 Å the amplitudes become stronger than those of (200) and (120) within the thickness of 500 Å. Thus it is reasonable that the image of O can always be observed.

Figs. 8 and 9 show magnified images of Cu_4O as observed in the two orientations [001] and [100] respectively. The calculated images and models obtained using the experimental data with the model
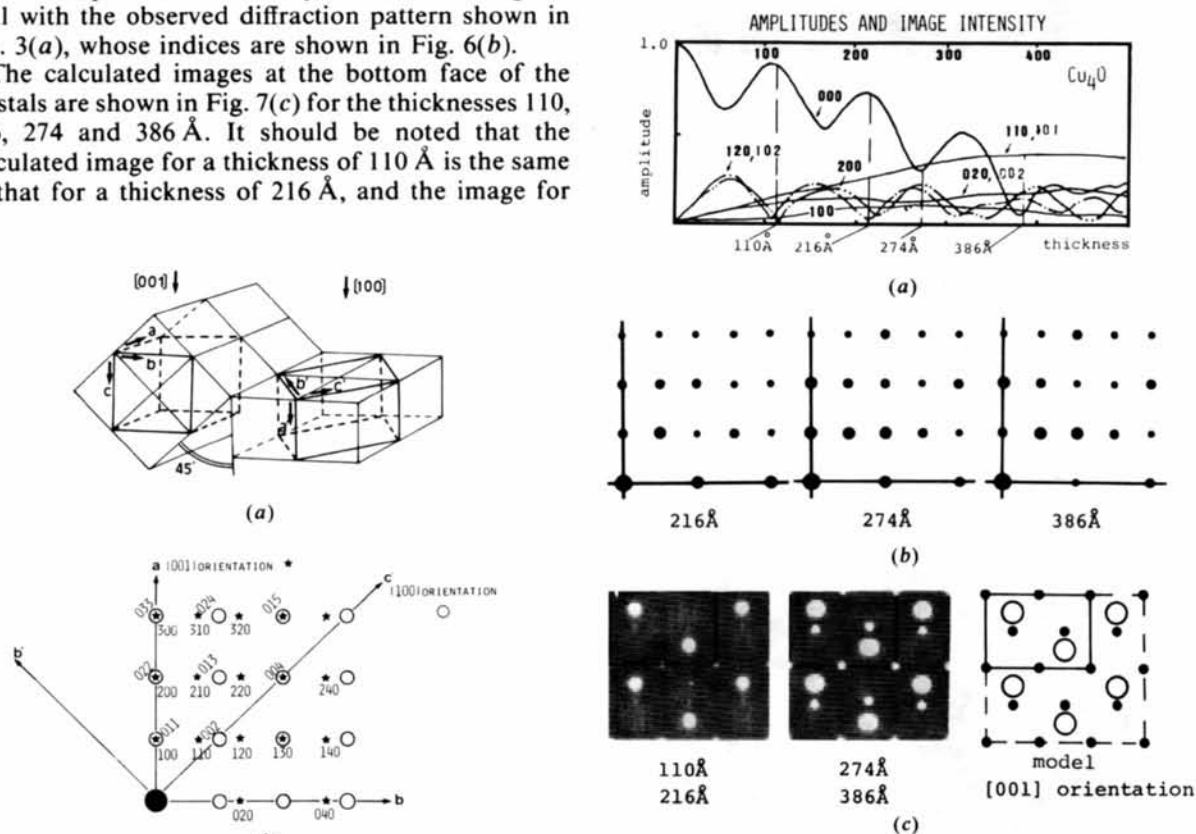

(a)

(b)

(c)

Fig. 7. (a) Thickness dependence of the amplitudes of diffracted electron waves from several atomic planes of Cu_4O. (b) Calculated intensity of electron diffraction patterns from Cu_4O crystals in [001] orientation for thickness values of 216, 274 and 386 Å. (c) Calculated intensity distribution of electron waves at the bottom surface of Cu_4O in [001] orientation and the projection of the atoms. Crystals of thickness 110 and 216 Å give identical images and only O atoms appear.

(a)

(b)

Fig. 6. (a) Perspective view of the Cu_4O lattice (thick lines) in [001] and [100] orientations and relation to the unit cell of Cu_2O (thin lines). The [100], [010] and [001] axes of Cu_4O are parallel to the [001], [1$\bar{1}$0] and [110] axes of Cu_2O, respectively. (b) Explanation of the electron diffraction patterns of Cu_4O crystals in [001] and [100] orientations, whose diffraction spots are represented by * and ○ respectively.

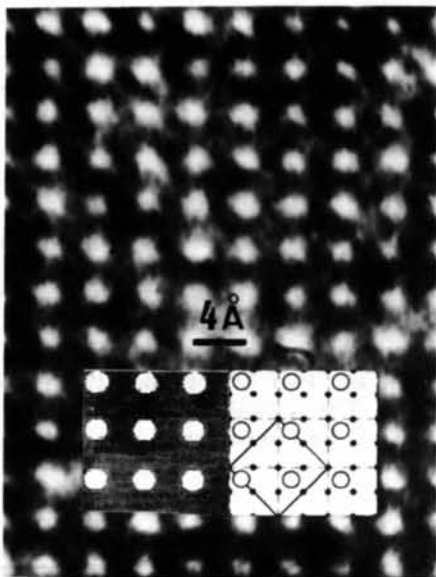of Cu_4O are shown at the bottom. The agreement between the observed and calculated images is fairly good.

Fig. 8. Observed and calculated images of the Cu_4O crystal in [001] orientation and the projection of Cu and O atoms. Calculated conditions: Δf (defocusing) = 1700 Å, C_s (spherical-aberration coefficient) = 0·67 mm, T (thickness) = 184 Å.
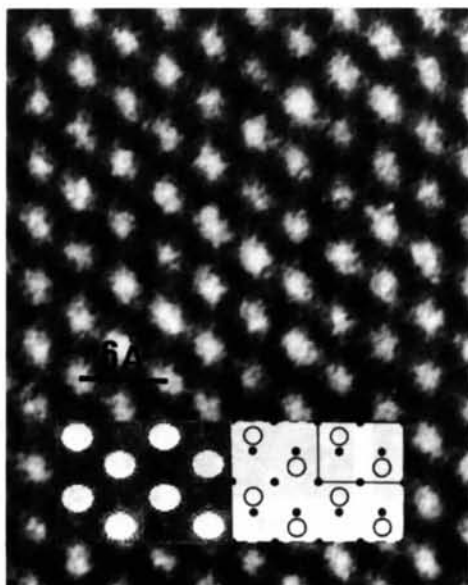

Fig. 9.   The same parameters as those shown in Fig. 8, but in [100] orientation with $T = 110$ Å.

5. Discussion and conclusion

During the initial stage of oxidation of copper crystals at 770–820 K in a vacuum of $10^{-1} \sim 10^{-3}$ Pa, a very thin layer of a metastable oxide with the chemical composition Cu_4O has been observed.

During the oxidation process, O atoms go into the copper lattice interstitially. As can be seen in Figs. 4(a) and 5(c), if both positions $(\frac{1}{4}, \frac{1}{4}, \frac{1}{4})$ and $(\frac{3}{4}, \frac{3}{4}, \frac{3}{4})$ in the unit cell of the copper lattice are occupied by O atoms, the Cu_2O crystal structure is formed. If only one O atom occupies the position $(\frac{1}{4}, \frac{1}{4}, \frac{1}{4})$ or $(\frac{1}{4}, \frac{1}{4}, \frac{3}{4})$ in the unit cell of the copper lattice as shown in Fig. 5(b), the Cu_4O crystal structure is formed. In the Cu_4O crystal structure, the positions of the O atoms are not the same as those in the Cu_2O structure and thus Cu_4O cannot easily be changed to Cu_2O by heating to the temperature where Cu_2O crystals normally grow. Allowing for the difference in the unit cell, the Cu_4O crystals seem to grow on the surface of the copper epitaxially with a relation similar to that of the Cu_2O crystals grown on a copper substrate, i.e. the [001], [$\bar{1}$01] and [110] axes of the Cu_4O crystal are parallel to the [100], [010] and [001] axes of the Cu_2O crystal respectively which are parallel to the [100], [010] and [001] axes of the copper.

The formation mechanism of Cu_4O crystals may not be much different from that of Cu_2O crystals grown on a clean copper surface. However, the surface of an electropolished copper film may be contaminated with some materials which act catalytically and thus Cu_4O crystals seem to be formed instead of Cu_2O.

References

ALLESSANDRINI, E. I. & FREEDMAN, J. F. (1963). Acta Cryst. 16, 54–57.
GARMON, L. B. & LAWLESS, K. R. (1966). Proceedings of the Sixth International Congress on Electron Microscopy, Kyoto, Vol. 1, pp. 541–542.
HOWIE, A. (1981). Inst. Phys. Conf. Ser. No. 61, ch. 9, pp. 419–424.
HOWIE, A. (1983). Proceedings of the Surface Science Electron Microscopy Workshop. Arizona Univ. In the press.
ISHII, M. & HASHIMOTO, H. (1967). Jpn. J. Appl. Phys. 6, 173–180.
SHIBAHARA, H. & HASHIMOTO, H. (1980). J. Appl. Cryst. 13, 591–596.